9606 *Biochemistry* **2009,** *48,* 9606–9617
DOI: 10.1021/bi900510f

BIOCHEMISTRY
including biophysical chemistry & molecular biology
Article

Nonproteolytic Induction of Catalytic Activity into the Single-Chain Form of Urokinase-Type Plasminogen Activator by Dipeptides†

Kenneth A. Bøtkjær,[‡,§,⊥] Aleksandra A. Byszuk,[‡,∥,⊥] Lisbeth M. Andersen,[‡] Anni Christensen,[‡] Peter A. Andreasen,*[,‡,§] and Grant E. Blouse[‡,@]

[‡]*Department of Molecular Biology, University of Aarhus, Aarhus, Denmark,* [§]*Danish-Chinese Centre for Proteases and Cancer, University of Aarhus, Aarhus, Denmark, and* [∥]*Faculty of Biochemistry, Biophysics and Biotechnology, Jagiellonian University, Krakow, Poland* [⊥]*These authors contributed equally to this work.* [@]*Present address: Catalyst Biosciences, 260 Littlefield Ave., South San Francisco, CA 94080.*

Received March 25, 2009; Revised Manuscript Received July 27, 2009

ABSTRACT: Serine proteases are initially synthesized as single-chain proenzymes with activities that are many orders of magnitude lower than those of the mature enzyme. Proteolytic cleavage of an exposed loop liberates a new amino terminus that inserts into a hydrophobic pocket and forms a stabilizing salt bridge with a ubiquitously conserved aspartate residue, resulting in a conformational change organizing the mature oxyanion hole. In a decisive 1976 work, Huber and Bode [Bode, W., and Huber, R. (1976) *FEBS Lett. 68*, 231−236] demonstrated that peptides sequentially similar to the new amino terminus in combination with a catalytic site inhibitor could specifically induce a trypsin-like conformation in trypsinogen. We now demonstrate that an Ile-Ile or Ile-Val dipeptide can induce limited enzyme activity in the single-chain zymogen form of urokinase-type plasminogen activator (uPA) or its K158A variant, which cannot be activated proteolytically. Furthermore, the slow formation of a covalent serpin−protease complex between single-chain uPA and PAI-1 is significantly accelerated in the presence of specific dipeptide sequences. The technique of using a dipeptide mimic as a surrogate for the liberated amino terminus further provides a novel means by which to covalently label the immature active site of single-chain uPA with a fluorescent probe, permitting fluorescence approaches for direct observations of conformational changes within the protease domain during zymogen activation. These data demonstrate the structural plasticity of the protease domain, reinforce the notion of "molecular sexuality", and provide a novel way of studying conformational changes of zymogens during proteolytic activation.

Serine proteases are secreted as zymogens, or pro-enzymes, having intrinsic catalytic activities orders of magnitude lower than those of their mature counterparts. The switch between a structural flexibility of the zymogen and the rigidity of the active protease domain is thought to play a central role in the control of enzyme activation. Proteolytic activation of secreted zymogens is consequently the key mechanism by which serine protease regulation proceeds in nature, allowing for strict control and rapid amplification of an activation signal (*1*). The intrinsic catalytic activity of a zymogen relative to that of the mature protease has generally been considered to be a problem of equilibrium between active and inactive conformations of the protease domain. The noncatalytic states of most zymogens are thought to persist through stabilization of the equilibrium toward an inactive conformation, in part by a conserved network of interactions involving the side chains of residues Ser32, His40, and Asp194, collectively termed the zymogen triad. Enzyme activation generally occurs by proteolytic cleavage of the peptide bond between residues 15 and 16 (chymotrypsin template numbering), resulting in a newly liberated amino terminus that readily inserts into a hydrophobic binding cleft in the catalytic domain forming a salt bridge to the side chain of Asp194, stabilizing the oxyanion hole in a catalytically productive conformation (Figure 1). Proteolytic activation of the enzyme triggers several key global conformational changes necessary for formation of a mature active site that are propagated throughout the activation domain, including residues within the activation loop (residues 16−21), the autolysis loop (residues 142−152), the oxyanion stabilizing loop (residues 184−193), and the S1 entrance frame (residues 216−223) (*1*−*3*).

In 1976, Bode and Huber (*4*) demonstrated that dipeptides analogous to the amino terminus of active trypsin (Ile-Val) can mimic the free amino terminus of the mature, active enzyme in the sense that they substitute for binding to the hydrophobic pocket within the activation domain of trypsinogen and form a salt bridge to Asp194. The term "molecular sexuality" was coined to describe this phenomenon in which the dipeptides can insert into the hydrophobic pocket and shift the conformational equilibrium of the single-chain, inactive trypsinogen toward that of the mature, two-chain protease. Evidence from X-ray crystallography demonstrated that the structure of a complex of trypsinogen

†This work was supported by grants from the Danish Cancer Society, the Danish Cancer Research Foundation, the Danish Research Agency, the Carlsberg Foundation, the Novo-Nordisk Foundation, the European Union, and the Danish National Research Foundation (to P.A. A.), the Danish Heart Association (to G.E.B.), and the University of Aarhus to (K.A.B.).

*To whom correspondence should be addressed: Department of Molecular Biology, University of Aarhus, Gustav Wied's Vej 10C, 8000 Aarhus C, Denmark. Telephone: +45 8942 5080. Fax: +45 8612 3178. E-mail: pa@mb.au.dk.

 Published on Web 08/25/2009

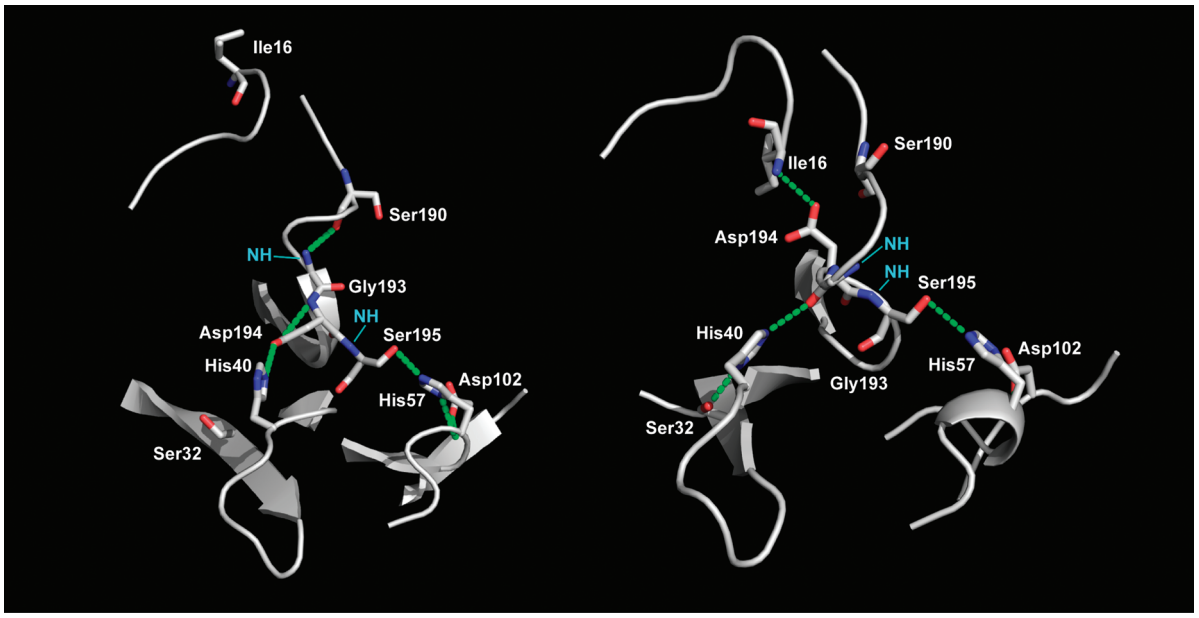

FIGURE 1: Structural aspects of activation of zymogens to catalytic serine proteases. Shown are parts of the three-dimensional structures of chymotrypsinogen (left) and chymotrypsin (right) depicted as ribbons. Shown as sticks are the side chains of the catalytic triad, His57, Asp102, and Ser195; the side chains of Ile16 and Asp194, with the salt bridge stabilizing the oxyanion hole in chymotrypsin; and the side chains of Ser32 and His40, which together with Asp194 form the zymogen triad and prevent stabilization of the oxyanion hole in chymotrypsinogen. The amido groups of Ser195 and Gly193, forming the oxyanion hole, are labeled with blue letters. These images were constructed in PyMol on the basis of the coordinates provided in PDB entries 1EX3 (*55*) and 1K2I (*56*), respectively.

with bovine pancreatic trypsin inhibitor (BPTI)[1] was almost indistinguishable from that of the trypsin−BPTI complex; however, exogenous Ile-Val peptide was required to induce the final stabilization of the autolysis loop (*5*). The addition of Ile-Val to a *p*-guanidinobenzoate−trypsinogen complex also yielded a circular dichroism spectrum that was identical to that of a *p*-guanidinobenzoate−trypsin complex (*6*). While these early studies failed to demonstrate that conformational changes in the zymogen could also reflect formation of a mature and functional catalytic site (*4*−*6*), a number of ensuing investigations have since characterized the effects of exogenous peptides on protease flexibility and demonstrated the induction of catalytic activity into trypsinogen through the binding of activating dipeptides, albeit with specificity constants (k_{cat}/K_M) for the hydrolysis of ester and amide substrates far below that of active trypsin (*7*−*12*).

It was later demonstrated that the molecular sexuality mechanism for nonproteolytic zymogen activation is in fact a viable strategy utilized in nature. Direct proof confirming the hypothesis was provided by crystallographic and kinetic studies showing that insertion of the amino terminus of staphylocoagulase into the Ile16 binding pocket of prothrombin is crucial for the nonproteolytic, allosteric activation of this protease (*13*). Biochemical studies have also shown that the amino-terminal Ile-Ala-Gly residues of streptokinase insert into the Ile16 binding pocket of plasminogen, which together with other interactions, preferentially stabilizes a catalytically active state of this single-chain zymogen. However, in the latter case, no structural proof for the mechanism is yet available (*14*, *15*).

Although bacterial cofactor-induced zymogen activation appears to effectively induce catalytic activity at levels reminiscent of the active protease (*13*, *16*−*19*), it remains unclear why a similar activation by exogenous dipeptides in trypsinogen is unable to realize full enzymatic activity (*7*). Thus far, the induction of catalytic activity in a binary adduct of a zymogen with an exogenous dipeptide has been demonstrated with trypsinogen only using synthetic ester and amide substrates (*6*−*12*). We have recently explored the possibility of nonproteolytic activation of the single-chain zymogen form of urokinase-type plasminogen activator (uPA), a serine protease that catalyzes the conversion of plasminogen to the active protease, plasmin (*20*). The existence of the single-chain zymogen form of uPA (pro-uPA) was first reported in the early 1980s (*21*−*23*), and pro-uPA appears to be the one predominating in blood and tissues in vivo (*24*). Several proteases, including plasmin (*20*), glandular kallikrein (*25*), matriptase (*26*), and hepsin (*27*), have now been reported to catalyze the activation of single-chain uPA. Nonetheless, pro-uPA is distinct from most other serine proteases in retaining an enzymatic activity that is reported to be approximately 250−1000-fold lower than that of the mature protease (*28*). A plausible explanation for the relatively high intrinsic activity of pro-uPA compared to that of trypsinogen is the fact that uPA is lacking the consensus zymogen triad, having alanine and tyrosine residues in place of Ser32 and His40, respectively (*3*, *29*). This characteristic of the zymogen also makes it susceptible to inhibition by the physiological uPA inhibitor, plasminogen activator inhibitor-1 (PAI-1), albeit at a significantly reduced rate (*30*, *31*). Therefore, further insight into the mechanism(s) of pro-uPA activation is of interest, especially in light of the established view that uPA is associated with tissue remodeling and abnormal expression is reflected in several pathological conditions, including rheumatoid arthritis, allergic

[1]Abbreviations: BSA, bovine serum albumin; BPTI, bovine pancreatic trypsin inhibitor; EGR-cmk, Glu-Gly-Arg-chloromethylketone; HBS, 30 mM HEPES (pH 7.4), 135 mM NaCl, and 1 mM EDTA; HBS-B, 30 mM HEPES (pH 7.4), 135 mM NaCl, 1 mM EDTA, and 0.1% bovine serum albumin; PAB, *p*-aminobenzamidine; PAI-1, plasminogen activator inhibitor-1; PBS, phosphate-buffered saline; PMSF, phenylmethanesulfonyl fluoride; S-2444, pyroGlu-Gly-Arg-*p*-nitroanilide; tPA, tissue-type plasminogen activator; uPA, urokinase-type plasminogen activator.

vasculitis, and xeroderma pigmentosum. In particular, uPA is central to the invasive capacity of malignant tumors (*20*), and pro-uPA activation has been highly correlated with tumor cell intravasation (*32*). Akin to all trypsin-like serine proteases, uPA has a highly conserved catalytic domain structure with variable surface-exposed loops around residues 37, 60, 97, 110, 170, and 185. In addition to the catalytic domain, uPA has an N-terminal extension consisting of a kringle domain and an epidermal growth factor domain. The latter domain functions in binding to the cell surface-anchored uPA receptor (uPAR) (*20*).

In this work, we demonstrate that dipeptides corresponding to the amino terminus of the mature protease can induce enzyme activity into the single-chain zymogen form of uPA in a manner comparable to prior observations with trypsinogen (*7*, *8*, *11*, *12*). However, the level of inducible catalytic activity relative to that of the active two-chain protease was found to be greater for pro-uPA−dipeptide adducts than previously reported for trypsinogen−dipeptide adducts against amide substrates (*7*, *10*). Moreover, we now present evidence that exogenous dipeptides confer significantly improved reactivity of pro-uPA with PAI-1, a surrogate macromolecular substrate, to within 2 orders of magnitude of that of the active two-chain enzyme. These results clearly demonstrate that, unlike previous work with trypsinogen (*4*−*6*), varying levels of enzyme activity may be imparted to a zymogen by small molecule exogenous modulators against not only small synthetic amide and ester substrates but also macromolecule substrates, improving our understanding of regulatory mechanisms for serine proteases.

EXPERIMENTAL PROCEDURES

uPA. Human two-chain uPA (tc-uPA) was purchased from Wakamoto (Tokyo, Japan). Recombinant human single-chain uPA was a gift from Abbott Laboratories. Pro-uPA was treated with 1 mM diisopropyl fluorophosphate to inactivate any residual two-chain activity. Labeling of uPA (25 μM) with EGR-cmk (1 mM) or 1,5-dansyl-EGR-cmk (1 mM) was conducted in phosphate-buffered saline (PBS) at 25 °C for 60 min. Labeling of single-chain uPA (12−20 μM) with EGR-cmk or 1,5-dansyl-EGR-cmk (10−20 mM) required the addition of 50 mM Ile-Ile dipeptide at 37 °C for 4 h. Excess inhibitor was removed by extensive dialysis against 20 mM citric acid and 50 mM NaCl (pH 4.5). Wild-type and mutant recombinant human single-chain uPA variants were expressed in HEK293T cells (*33*), cultured in the presence of 5 μg/mL BPTI, and in some cases purified as previously described (*33*).

PAI-1. Human PAI-1 was expressed with an N-terminal His_6 tag and purified from *Escherichia coli* cells as described previously (*34*, *35*). P9-Cys PAI-1 was labeled with *N*,*N*′-dimethyl-*N*-(iodoacetyl)-*N*′-(7-nitrobenz-2-oxa-1,3-diazol-4-yl)ethylenediamine (IANBD amide) as described previously (*36*) with a labeling efficiency that was typically 1−1.2 mol of NBD/mol of PAI-1 variant. Latent PAI-1 that accumulated during the labeling reaction was subsequently removed by affinity chromatography on immobilized β-anhydrotrypsin, binding only active PAI-1. The final P9-NBD-labeled preparations were shown to be >98% active by sodium dodecyl sulfate−polyacrylamide gel electrophoresis (SDS−PAGE) analysis (*36*).

Antibodies. The following monoclonal anti-human uPA antibodies were employed: mAb-112 and FAb-112 (*37*).

Miscellaneous Materials. Upain-1-D1D2, a fusion product between the disulfide bridge-constrained CSWRGLENHRMC peptide and the two N-terminal domains of M13 phage coat protein p3g, was prepared as described previously (*38*). The following materials were purchased from the indicated sources: pyroGlu-Gly-Arg-*p*-nitroanilide (S-2444) from Chromogenix (Mölndal, Sweden); BPTI, phenylmethanesulfonyl fluoride (PMSF), *p*-aminobenzamidine (PAB), and amiloride from Sigma-Aldrich (Steinheim, Germany); and Ile-Ile, Ile-Val, Asp-Val, and Arg-Val dipeptides from Bachem (Bubendorf, Switzerland).

Amidolytic Assay of uPA Activity. Rates for the uPA-catalyzed hydrolysis of the chromogenic substrate S-2444 were measured at 37 °C in 30 mM HEPES, 135 mM NaCl, 1 mM EDTA, and 0.1% BSA (pH 7.4) (HBS-B) with 1 μg/mL BPTI over a range of substrate concentrations (0−6 mM). For amidolytic assays in the presence of mAb-112, 5 nM tc-uPA or 150 nM pro-uPA was preincubated with or without 50 mM dipeptide in the presence or absence of 225 nM mAb-112 together with 1 μg/mL BPTI for 30 min at 25 °C prior to initiation of the hydrolysis reactions at 37 °C to determine the kinetic constants. Initial rates of S-2444 hydrolysis were monitored at 405 nm. Initial rates of substrate hydrolysis were plotted against the substrate concentration, and data were fit to eq 1 to determine the individual k_{cat} and K_M parameters.

$$v = \frac{k_{cat}[\text{uPA}][\text{S}]}{K_M + [\text{S}]} \quad (1)$$

Determination of the Inhibition Constants (K_i) for the Inhibition of uPA and Pro-uPA. Inhibition constants (K_i) for the inhibition of purified uPA or pro-uPA in the presence of competitive inhibitors (upain-1-D1D2, amiloride, or PAB) under equilibrium conditions were determined with a fixed concentration of uPA (4.0 nM) or pro-uPA (150 nM) that was preincubated in a 0.2 mL volume of HBS-B at 37 °C and pH 7.4 with various concentrations of the inhibitors (0−6 mM) and in presence or absence of dipeptides prior to the addition of the chromogenic substrate, S-2444 (250 μM for uPA and 500 μM for pro-uPA). The initial reaction velocities were monitored at an absorbance of 405 nm. Apparent equilibrium inhibition constants (K_i^{app}) were subsequently determined from the nonlinear regression analyses of plots for V_i/V_0 versus $[I]_0$ using a variation of the Morrison equation as described previously (*38*):

$$V_i/V_0 = 1 - \left[[E]_0 + [I]_0 + K_i^{app} - \sqrt{([E]_0 + [I]_0 + K_i^{app})^2 - 4[E]_0[I]_0}\right]/2[E]_0 \quad (2)$$

where V_i and V_0 are the reaction velocities in the presence and absence of inhibitor, respectively, $[E]_0$ and $[I]_0$ are the total protease and inhibitor concentrations, respectively, and K_i^{app} represents the apparent inhibition constant in the presence of chromogenic substrate. The true K_i was subsequently determined by correcting for the competitive effect of the substrate S using the relationship

$$K_i = K_i^{app}/(1+[S]_0/K_M) \quad (3)$$

Fluorescence Emission Spectroscopy with Dansyl-Labeled Pro-uPA. Fluorescence emission spectra of dansyl-labeled pro-uPA (100 nM) were recorded using a SPEX-3 spectrofluorimeter equipped with a Peltier temperature controller maintaining the measurement and incubation temperatures at 25 °C. Fluorescence experiments were conducted using semimicro

(0.5 cm × 1.0 cm) quartz cuvettes in a HBS reaction buffer containing 0.1% PEG 8000 to prevent adsorption of protein to the quartz surface. The excitation wavelength used for studying the fluorescence of dansyl-EGR-pro-uPA was 335 nm, and the emission spectra were scanned from 450 to 650 nm using an excitation bandwidth of 5 or 10 nm and an emission bandwidth of 5 nm. Emission spectra were recorded prior to and after the addition of plasmin or various concentrations of dipeptides as indicated for each individual experiment. Results are presented as the averaged spectra of at least three independent titrations. All individual emission spectra were collected as averages of three to five emission scans using a 1.0 s integration over a 1.0 nm step resolution and corrected for background fluorescence and dilution effects, which were typically less than 5%.

Fluorescence Emission Spectroscopy with P9-NBD-PAI-1. Reactions between 50 nM P9-NBD-PAI-1 and 0−16 μM pro-uPA in the presence and absence of 50 mM dipeptides were assessed with a PTI QM-4CW spectrofluorimeter equipped with a Peltier temperature controller maintaining the measurement and incubation temperatures at 25 °C. Samples were diluted in HBS reaction buffer containing 0.1% PEG 8000. The reaction was followed over time with an excitation wavelength of 480 nm and an emission wavelength of 522 nm. The obtained reaction traces were fit to a single-exponential equation, which provided a k_{obs} value for each pro-uPA concentration. The dependence of the obtained k_{obs} values on the concentration of pro-uPA is described by a single rectangular hyperbola and gives the parameters k_{lim} and K_M for the reaction between PAI-1 and pro-uPA:

$$k_{obs} = \frac{k_{lim}[uPA]}{K_M + [uPA]} \quad (4)$$

Stopped-Flow Kinetics of P9-NBD-Labeled PAI-1. Stopped-flow fluorimetry was performed on an Applied Photophysics SX.18MV instrument with a thermostated syringe chamber as described previously (*36*). The fluorescence change accompanying the reaction of 50 nM P9-NBD-labeled PAI-1 with 0.25−6 μM uPA in the presence or absence of 50 mM dipeptides was monitored with an excitation wavelength at 480 nm and an emission filter (Oriel 51300) with a cutoff below 515 nm. The reaction temperature was 25 °C, and the buffer was a HBS reaction buffer containing 0.1% PEG 8000. Stopped-flow reaction traces were fit to a single-exponential function, yielding the pseudo-first-order rate constant (k_{obs}). The obtained k_{obs} values were plotted against the protease concentration and fitted to the rectangular hyperbola function described in eq 4, which gives a k_{lim} and a K_M for the reaction between PAI-1 and uPA.

Analysis of Formation of a Complex between Single-Chain uPA and PAI-1 by SDS−PAGE. Formation of a complex between single-chain uPA and PAI-1 was followed by preincubating 3 μM single-chain uPA, in HBS with 0.1% PEG 8000 and 1 μg/mL BPTI, with or without 50 mM dipeptide in the presence or absence of preincubated FAb-112 in a 1.5-fold molar excess for 30 min at 25 °C. The reaction was started by addition of PAI-1 to a final concentration of 6 μM. After incubation for variable lengths of time, samples were taken and the reaction was stopped by addition of PMSF to a final concentration of 1 mM and boiling for 5 min. The reaction products were analyzed by SDS−PAGE under reducing conditions. The resulting protein bands were visualized with Coomassie Brilliant Blue staining. Relative amounts of complex were quantified by densitometric scanning using Quantity One (Bio-Rad Laboratories, Hercules, CA). Reaction rates were evaluated as k_{obs}, the pseudo-first-order rate constant describing the monoexponential approach to complete inhibition, by fitting the data points to eq 5

$$\frac{[AB]_t}{[AB]_{max}} = 1 - e^{k_{obs}t} \quad (5)$$

where $[AB]_t$ is the amount of complex formed between pro-uPA and PAI-1 at time t, $[AB]_{max}$ is the maximal amount of complex that can be formed, and t is the reaction time.

RESULTS

Effect of Dipeptides on the Peptidolytic Activity of Single-Chain and Two-Chain uPA. We determined the effect of dipeptides Ile-Ile and Ile-Val on the turnover of the chromogenic substrate S-2444 by single-chain and two-chain uPA. These dipeptides correspond to the N-terminus of the two-chain form of uPA from human (Ile-Ile) or other mammals (Ile-Val). As controls, we have used two irrelevant dipeptides, Arg-Ile and Asp-Val, which have the N-terminal isoleucine substituted with an arginine and asparagine residue, respectively. We selected a dipeptide concentration of 50 mM, which in preliminary experiments was shown to confer near-optimal effects. In all assays, 1 μg/mL BPTI was added to prevent any potential contaminating proteases from cleaving and activating pro-uPA. As expected, the activity of the preparation of pro-uPA was much lower than that of active, two-chain uPA. While the K_M values for hydrolysis of S-2444 were indistinguishable from that of uPA, the k_{cat} value for pro-uPA was 1000-fold lower than that observed for two-chain uPA (Figure 2 and Table 1). The values for uPA were in agreement with those previously reported (*38*). Although precautions were taken to limit any two-chain uPA in the pro-uPA preparation, we cannot be certain that the hydrolysis observed with pro-uPA represents true endogenous activity but rather may reflect a small contamination with two-chain uPA. Nonetheless, the Ile-Ile and Ile-Val dipeptides conferred a remarkable increase in the catalytic activity of single-chain uPA, showing approximately 20- and 80-fold increases in k_{cat}, respectively (Figure 2 and Table 1). The K_M value for pro-uPA in the presence of the dipeptides was clearly higher than in the absence and much higher than that found for two-chain uPA, demonstrating that it represents an authentic increase in the endogenous activity of single-chain uPA and not a contamination with two-chain uPA. There was no effect of control dipeptide Arg-Ile or Asp-Val on single-chain uPA. In reactions evaluating the noncleavable K158A pro-uPA variant, the addition of specific and control dipeptides produced results similar to those with wild-type pro-uPA, again showing that the increased activity in the presence of the dipeptides was not due to cleavage by contaminating proteases. The addition of both the specific and control dipeptides only slightly reduced the K_M and k_{cat} values for two-chain uPA.

We have previously described a monoclonal antibody, mAb-112, that binds with high affinity to the autolysis loop of the zymogen form of uPA, but poorly to active, two-chain uPA. When bound by mAb-112, pro-uPA becomes locked in a zymogen-like state even after complete proteolytic activation, thus stabilizing an inactive oxyanion hole (*37*). The poor affinity for active uPA was therefore proposed to be a consequence of the rigidity of the active protease domain, only transiently existing in a zymogen-like conformation (*37*). We have now used mAb-112 as a measure of the flexibility of the activation domain in the

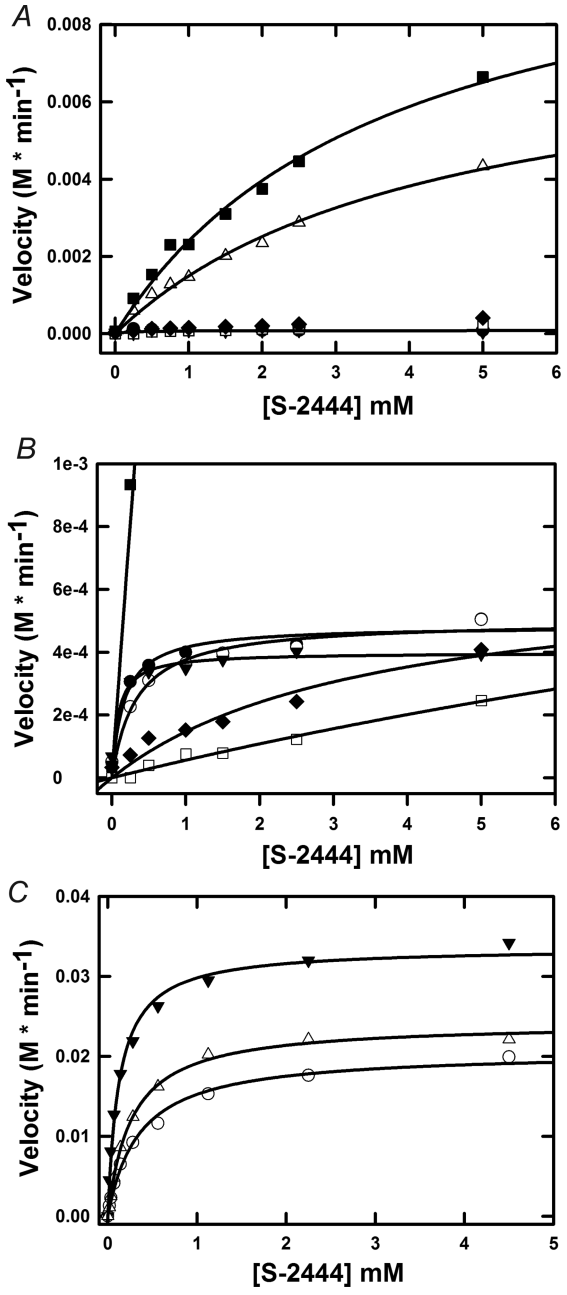

FIGURE 2: Effect of dipeptides on S-2444 hydrolysis catalyzed by single-chain and two-chain uPA. (A) The initial rates of S-2444 hydrolysis were determined at various S-2444 concentrations, in the presence of 150 nM single-chain uPA and with 50 mM Ile-Ile (△), 50 mM Ile-Val (■), 50 mM Arg-Ile (○), 50 mM Asp-Val (●), 225 nM mAb-112 and 50 mM Ile-Val (◆), and 225 nM mAb-112 and 50 mM Ile-Ile (□) or in the absence of dipeptides (▼). (B) Close-up of the graph in panel A, zooming in on the data without peptide addition (▼) or with addition of 50 mM Asp-Val (●), 50 mM Arg-Ile (○), 225 nM mAb-112 and 50 mM Ile-Val (◆), and 225 nM mAb-112 and 50 mM Ile-Ile (□). Also shown are the data for the addition of 50 mM Ile-Val (■). (C) Initial rates of S-2444 hydrolysis in the presence of 5 nM uPA and 50 mM Ile-Ile (△) and 50 mM Arg-Ile (○) or in the absence of dipeptides (▼). The hydrolysis rates were plotted vs the S-2444 concentration. Curves were fitted to the data points according to eq 1 (see Experimental Procedures) to determine K_M and k_{cat} values. The figure shows the result of one representative experiment for each condition. The results of a larger number of experiments are listed in Table 1.

presence of activating dipeptides. As shown in Figure 2, mAb-112 clearly inhibits nearly all of the enzymatic activity induced by the addition of the activating dipeptides, Ile-Ile and Ile-Val, suggesting that the autolysis loop likely remains more flexible and zymogen-like than would be expected for proteolytically activated uPA. Due to the fact that we were unable to reach saturation within the solubility limit of the substrate, kinetic parameters could not be reliably calculated for the mAb-112-inhibited reactions.

Effects of Competitive Inhibitors on Single-Chain and Two-Chain uPA in the Absence and Presence of Dipeptides. To further characterize the dipeptide-activated form of single-chain uPA, we measured the sensitivity of the dipeptide-activated zymogen to competitive uPA inhibitors. PAB is a general, competitive inhibitor of serine proteases (*39*), while amiloride is an inhibitor of Na^+ channels that by chance was found to inhibit uPA, but not the closely related tissue-type plasminogen activator (tPA) (*40*). Upain-1 is a dodecapeptide, which is a specific competitive inhibitor of human uPA (*38*, *41*). The K_i values measured for inhibition of two-chain uPA by these compounds (Table 2) were in agreement with those previously reported (*38*−*40*), all being in the low micromolar range. However, the activity of dipeptide-activated pro-uPA could not be inhibited by PAB or amiloride at concentrations as high as 5 mM, and the K_i value for inhibition of the dipeptide-activated pro-uPA by upain-1-D1D2 was nearly 100 μM, compared to ~2 μM for two-chain uPA. The presence of the dipeptides had only minor effects on the observed K_i values for inhibition of two-chain uPA (Table 2). Thus, although having limited enzymatic activity, the dipeptide-activated pro-uPA exhibited a significantly reduced susceptibility to competitive inhibitors targeting the S1 specificity pocket of the protease. On the other hand, reactions with the macromolecular inhibitor, upain-1-D1D2, which has an extended binding interface bridging the S1 and S2 pockets, the oxyanion hole, and an exosite on the 37 and 60 loops (*41*), resulted in an approximately 40-fold reduction in K_i compared to that of two-chain uPA.

Dipeptides Induce a Conformational Change in Single-Chain uPA. To be able to directly observe the conformational change associated with single-chain uPA activation in the presence of dipeptides, we developed a novel method for specific labeling of Ser195 in pro-uPA with a fluorescent probe. We took advantage of the fact that the Ile-Ile dipeptide shifts the equilibrium from an inactive toward an active protease conformation in the absence of proteolytic cleavage. Following a strategy previously employed in the case of prothrombin and plasminogen (*42*, *43*) and most recently by us with pro-uPA (*37*), we labeled Ser195 and His57 of single-chain uPA with the fluorescent and irreversible active site inhibitor, dansyl-EGR-cmk, in the presence of the Ile-Ile dipeptide. Upon removal of the dipeptide, the enzyme reverts to the inactive but now dansyl-labeled zymogen conformation, as judged from the fact that its K_D for binding to the monoclonal antibody mAb-112, specific for the inactive zymogen form of uPA, was unchanged and the fluorescence spectrum is clearly different from that of dansyl-labeled two-chain uPA (*37*). The labeled pro-uPA could be converted to a two-chain form by plasmin, but the activity after cleavage remained less than 1% of that of unlabeled two-chain uPA, demonstrating effective labeling of the active site (data not shown).

Plasmin cleavage of the dansyl-EGR-cmk-labeled single-chain uPA resulted in a quench and red shift of the fluorescence emission spectrum from 543 ± 5 to 568 ± 3 nm (n = 3) (Figure 3A). The change in the spectrum occurred with a time course that was indistinguishable from the time course of induction of catalytic activity (Figure 3B). We next demonstrated

Table 1: Effect of Dipeptides on the Catalytic Activity of Single-Chain uPA and Two-Chain uPA toward the Chromogenic Substrate S-2444[a]

protease	k_{cat} (min^{-1})	K_M (mM)	k_{cat}/K_M (M^{-1} s^{-1})	$\Delta G_T^{\ddagger b}$ (kcal/mol)
pro-uPA	0.73 ± 0.39	0.10 ± 0.02	$(1.2 \pm 0.7) \times 10^2$	15.2
pro-uPA with Ile-Ile	14.5 ± 4.4^c	4.0 ± 0.6^c	$(6.0 \pm 2.0) \times 10^{1c}$	15.7
pro-uPA with Ile-Val	56.6 ± 4.0^c	6.1 ± 2.2^c	$(1.5 \pm 0.6) \times 10^{2c}$	15.1
pro-uPA with Arg-Ile	0.31 ± 0.24	0.16 ± 0.15	$(3.2 \pm 3.9) \times 10^1$	16.0
pro-uPA with Asp-Val	0.14 ± 0.04	0.18 ± 0.02^c	$(1.3 \pm 0.4) \times 10^{1c}$	16.6
K158A pro-uPA	0.65 ± 0.06	0.08 ± 0.03	$(1.4 \pm 0.5) \times 10^2$	15.2
K158A pro-uPA with Ile-Ile	2.3 ± 0.6^c	2.2 ± 1.0^c	$(1.7 \pm 0.9) \times 10^{1c}$	16.4
K158A pro-uPA with Ile-Val	29.3 ± 0.8^c	5.0 ± 0.7^c	$(9.7 \pm 1.4) \times 10^{1c}$	15.4
K158A pro-uPA with Arg-Ile	0.35 ± 0.03^c	0.08 ± 0.06	$(7.3 \pm 5.5) \times 10^{1c}$	15.5
tc-uPA	773 ± 391	0.13 ± 0.01	$(9.9 \pm 5.1) \times 10^4$	11.1
tc-uPA with Ile-Ile	530 ± 275	0.18 ± 0.07	$(4.9 \pm 3.2) \times 10^4$	11.5
tc-uPA with Arg-Ile	601 ± 97	0.32 ± 0.04^c	$(3.1 \pm 0.6) \times 10^{4c}$	11.8

[a]Means and standard deviations are indicated for each value. Michaelis constants (K_M and k_{cat}) are reported as the averages ± the standard deviation of three to six independent experimental determinations. [b]Values for the transition state stabilization energy ($\Delta G_T^{\ddagger}$) were calculated from the k_{cat}/K_M values using the relationship $\Delta G_T^{\ddagger} = -RTln[(h/k_BT/h)(k_{cat}/K_M)]$, where k_B is Boltzmann's constant, h is Planck's constant, T is temperature, and R is the gas constant. [c]Significantly different from control in a t test with $p < 0.01$.

Table 2: Effect of Inhibitors on the Activity of Single-Chain uPA and Two-Chain uPA in the Absence and Presence of Dipeptides[a]

	pro-uPA K_i (μM)			tc-uPA K_i (μM)		
dipeptide	PAB	amiloride	upain-1	PAB	amiloride	upain-1
none	nm[b]	nm[b]	nm[b]	39.5 ± 11.2	5.0 ± 0.8	2.2 ± 0.1^c
Ile-Ile	nm[b]	nm[b]	95.4 ± 12.5^d	33.9 ± 4.6	6.8 ± 0.6	3.6 ± 2.7
Asp-Val	nm[b]	nm[b]	nm[b]	34.8 ± 3.1	5.1 ± 1.1	3.4 ± 2.8

[a]Means and standard deviations are indicated for each value. The inhibition constants (K_i) are reported as the averages ± standard deviation of three independent experimental determinations. [b]No measurable inhibition at inhibitor concentrations of up to 5 mM was observed. [c]This K_i value is taken from ref *38*. [d]Significantly different from control in a t test with $p < 0.005$.

that addition of the Ile-Ile peptide to the dansyl-EGR-pro-uPA produced a shift in the fluorescence emission spectrum identical to that produced by plasmin cleavage (Figure 4A). However, significantly lower concentrations of the dipeptide were required to produce the shift in the fluorescence emission spectrum associated with the maximal conformational change effect compared to that needed to induce catalytic activity in underivatized pro-uPA (Figure 4B). As shown in Figure 4B, approximately 275-fold more Ile-Ile dipeptide was required for the induction of maximal catalytic activity relative to that required for producing the full shift in fluorescence (compare $K_{0.5}$ values of 45.6 ± 5.3 mM and 165.8 ± 53.2 μM for induction of uPA activity and fluorescence emission, respectively). These findings demonstrate that the dipeptide activation of single-chain uPA is directly coupled to a conformational change similar to that occurring upon proteolytic activation; however, the labeling of the active site may facilitate the conformational change in the sense that it occurs at dipeptide concentrations lower than those required for unlabeled single-chain uPA. A likely explanation is that in the case where the dansyl inhibitor is already bound to the active site, the energy barrier required for the conformational transition is lower relative to that which must be overcome when there is no inhibitor or substrate present in the active site.

Dipeptides Increase the Rate of Reaction between Single-Chain uPA and PAI-1. Whereas the inhibitory reaction between active two-chain uPA and PAI-1 occurs with a second-order rate constant of ~5×10^6 M^{-1} s^{-1} (*36*, *44*), the reaction with single-chain uPA is reported to be at least 1000-fold slower (*30*, *31*). Because of the mechanistic nature of serpin inhibition, in which proteolytic cleavage of the reactive loop is a central step (*45*), PAI-1 also served as a surrogate macromolecular substrate for evaluation of dipeptide-induced activation of pro-uPA. We have now estimated the effect of dipeptides on the reaction between PAI-1 and pro-uPA. Initially, we studied the reaction with micromolar concentrations of both components and estimated the rates of complex formation by SDS−PAGE. The SDS−PAGE analysis was performed under reducing conditions to ensure that the observed complexes were those of PAI-1 and single-chain, not two-chain, uPA. Under reducing conditions, a covalent single-chain uPA−PAI-1 complex will migrate as an $M_r \sim 100000$ band, while a covalent two-chain uPA−PAI-1 complex will migrate as two bands, at $M_r \sim 80000$ and $M_r \sim 20000$. Given the saturating conditions of PAI-1 used in the assay, the pseudo-first-order rate of inhibition could be quantified by fitting the increasing density of the single-chain uPA−PAI-1 complex. Both the Ile-Ile and Ile-Val dipeptides were found to increase the apparent first-order rate constant for the reaction between PAI-1 and pro-uPA ~25-fold, while there was no effect when the Asp-Val or Arg-Ile dipeptide was used (Figure 5 and Table 3). Similar to our observations with the tripeptide *p*-nitroanilide substrate, the addition of a molar excess of FAb-112 prevented the inhibition of dipeptide-activated pro-uPA by PAI-1 (Figure 5).

With micromolar concentrations, SDS−PAGE does not allow sufficient resolution of the fast time course for two-chain uPA reactions with PAI-1. To evaluate these effects and directly compare kinetic constants for PAI-1 inhibition, we have used a well-described fluorescence model for monitoring the transient reaction kinetics of PAI-1 inhibition of target proteases by means of following the insertion of the reactive center loop with a fluorescent probe (*46*). This methodology provided a sensitive approach for measuring the effects of dipeptides on the rate of reactive center loop insertion when the labeled PAI-1 was reacted with single-chain or two-chain uPA in the presence or absence of activating dipeptides. For this model system, the PAI-1 molecule was labeled at the P9 residue with NBD to follow reactive center loop insertion by fluorescence spectroscopy. The slow reactions of pro-uPA in the presence or absence of activating dipeptides were conducted in cuvettes using the time-based data acquisition mode, whereas the fast reactions with two-chain uPA were best suited for a stopped-flow approach. Consistent with earlier

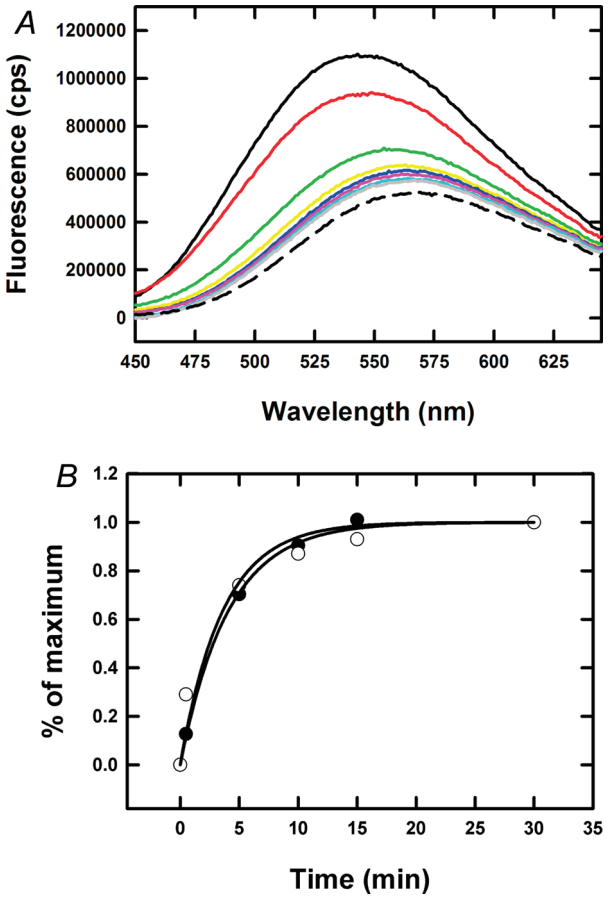

FIGURE 3: Effect of plasmin cleavage on the emission spectrum of dansyl-EGR-cmk-labeled single-chain uPA. (A) Dansyl-EGR-cmk-labeled single-chain uPA (100 nM) was incubated with 10 nM plasmin for 0 (black), 0.5 (red), 5 (green), 10 (yellow), 15 (blue), 30 (pink), 60 (light blue), and 120 min (grey). The plasmin activity was then stopped by addition of 30 nM BPTI. Fluorescence emission spectra were recorded with an excitation wavelength of 335 nm. The fluorescence emission spectrum recorded for dansyl-EGR-cmk-labeled two-chain uPA is shown with a dotted line. (B) Single-chain uPA (100 nM) was incubated with 10 nM plasmin for the indicated time periods. Plasmin activity was quenched by the addition of 30 nM BPTI and the uPA activity measured as the initial rate of hydrolysis of 0.75 mM S-2444. The fractional change in uPA activity (●) and the fractional change in the integrated fluorescence emission (○) were plotted vs incubation time. Reaction progress curves were fit using the monoexponential expression $y = 1 - e^{kt}$, where y is the observed fractional change, t is the time, and k is the first-order rate constant describing the observed fractional change in activity or fluorescence emission (k was determined to be 0.24 min^{-1} for the change in uPA activity and 0.39 min^{-1} for the change in fluorescence emission). Shown are representative experiments for a total of three independent replicate experiments.

observations (*30*, *31*), we demonstrated a >10000-fold lower rate of inhibition for single-chain uPA relative to two-chain uPA (Table 4). Single-chain uPA in the presence of the activating dipeptides, Ile-Ile and Ile-Val, was inhibited approximately 20 and 45 times faster than in the absence of the dipeptides or in the presence of the control dipeptide Asp-Val (Figure 6 and Table 4). Interestingly, the increases in catalytic activity were exclusively associated with enhancements in the overall limiting rate of the inhibition reaction (k_{lim}), while negligible effects on K_M were observed. Control reactions with two-chain uPA in the presence of the dipeptides indicated that there were no significant effects on the inhibition reaction (Table 4).

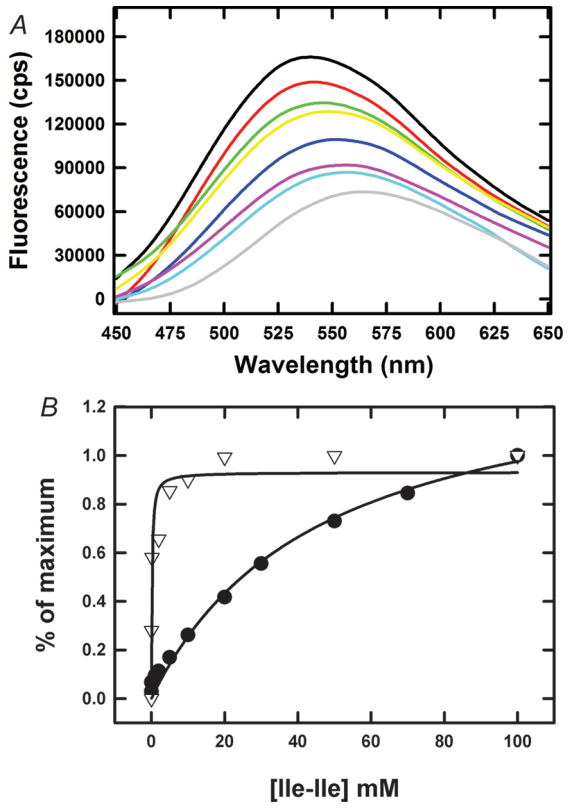

FIGURE 4: Effect of Ile-Ile on the fluorescence emission spectra of dansyl-EGR-cmk-labeled single chain uPA. (A) The fluorescence emission spectra of 100 nM dansyl-EGR-cmk-labeled single-chain uPA were recorded after a 15 min preincubation in the absence (black) and presence of 100 μM (red), 500 μM (green), 1 mM (yellow), 5 mM (blue), 10 mM (pink), 50 mM (light blue), and 100 mM Ile-Ile dipeptide (gray). (B) In parallel, 100 nM single-chain uPA was preincubated for 15 min with a range of Ile-Ile concentrations, after which the uPA activity was measured as the initial rate of hydrolysis of 3 mM S-2444. The fractional change in uPA activity (●) and the fractional change in the integrated fluorescence emission (▽) were plotted vs Ile-Ile dipeptide concentration. Data were analyzed using the expression $y = F_{max}[\text{Ile-Ile}]/(K_{0.5} + [\text{Ile-Ile}])$, where y is the observed fractional change, F_{max} is the maximal fractional change (uPA activity or fluorescence emission), [Ile-Ile] is the concentration of the Ile-Ile dipeptide, and $K_{0.5}$ is the half-maximal amount of Ile-Ile required for the observed fractional change in activity or fluorescence emission. The fitting routine yielded $K_{0.5}$ values of 45.6 ± 5.3 mM and 165.8 ± 53.2 μM for induction of uPA activity and fluorescence emission, respectively. Shown are representative experiments from a total of three independent replicates. Equivalent fluorescence emission spectra were observed with the Ile-Val dipeptide, whereas the Asp-Val dipeptide had no effect on the emission spectrum.

DISCUSSION

We demonstrate here that exogenously added dipeptides corresponding to the first two N-terminal amino acids in the mature enzyme can stimulate limited catalytic activity in the single-chain zymogen form of uPA. Although no measurable catalytic activity could be induced in trypsinogen with high Ile-Val concentrations in the original studies on the concept of molecular sexuality by Bode and Huber (*4*), several later studies have indeed shown that the trypsinogen−Ile-Val binary adduct has modest catalytic activity, although the induced catalysis for hydrolysis of amide and ester substrates was at best 10^4-fold lower than that of active trypsin (*7*, *10*). The preset studies expand upon the earlier work by demonstrating that a measurable activity of the single-chain uPA adducts with the two activating dipeptides, Ile-Ile and Ile-Val, more closely approaches the

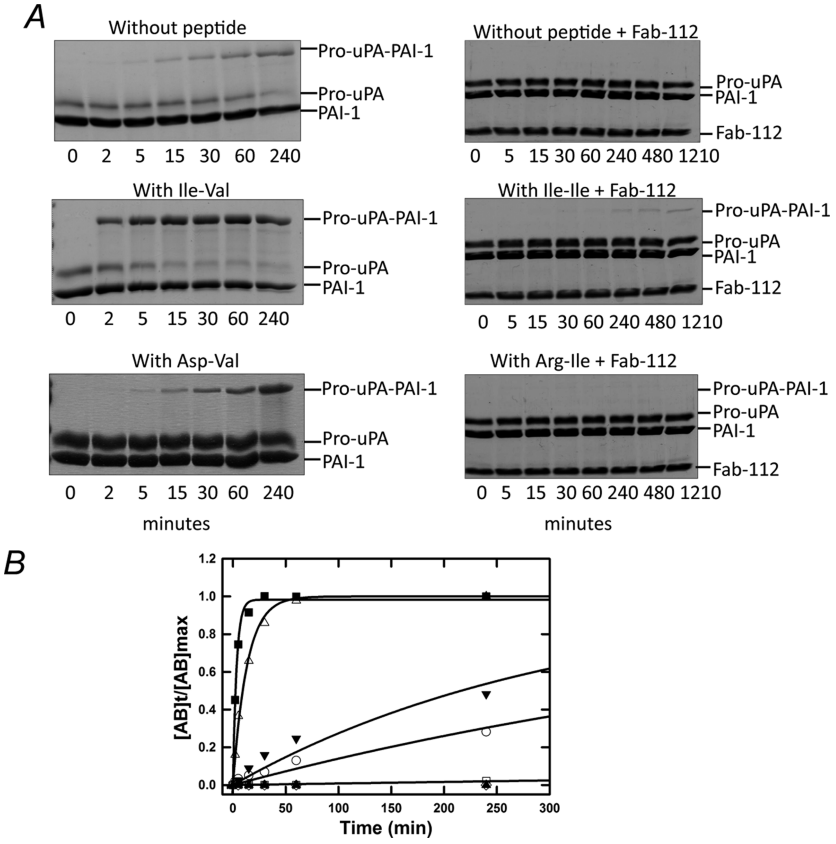

FIGURE 5: Time course of formation of the complex between single-chain uPA and PAI-1, as analyzed by SDS−PAGE under reducing conditions. (A) Single-chain uPA (3 μM) was incubated with 6 μM PAI-1 at room temperature, with or without 50 mM dipeptide (Ile-Ile, Ile-Val, Arg-Ile, or Asp-Val) and a molar excess of FAb-112 as indicated. Reactions were stopped at varying time points via addition of PMSF to a final concentration of 1 mM and boiling in reducing sample buffer. The products were analyzed via SDS−PAGE under reducing conditions. (B) The relative densities of the single-chain uPA−PAI-1 complex bands were estimated by densitometric scanning of the gels, and the values for the fraction of formed complex between single-chain uPA and PAI-1 were plotted vs time of incubation in the presence of Arg-Ile (○), Ile-Ile (△), Ile-Val (■), Ile-Ile and FAb-112 (□), Arg-Ile and FAb-112 (◇), and FAb-112 (▲) or in the absence of dipeptides (▼). The k_{obs} values for a monoexponential approach to complete inhibition were calculated by nonlinear fitting of the data points to the equation $[AB]_t/[AB]_{max} = 1 - e^{k_{obs}t}$ (also see Experimental Procedures). The result of a representative experiment is shown. The results of a larger number of experiments are listed in Table 3.

Table 3: Observed Rates of Reaction between Single-Chain uPA and PAI-1 in the Absence and Presence of Dipeptides[a]

dipeptide	k_{obs} (min^{-1})[b]
none	$(2.8 \pm 0.6) \times 10^{-3}$
Ile-Ile	$(6.3 \pm 1.2) \times 10^{-2}$
Ile-Val	$(1.4 \pm 0.4) \times 10^{-1}$[c]
Arg-Ile	$(1.4 \pm 0.3) \times 10^{-3}$
Asp-Val	$(4.6 \pm 1.5) \times 10^{-3}$

[a]See also Figure 5. Means and standard deviations are indicated for each value. The observed pseudo-first-order rate constants (k_{obs}) are reported as the averages ± standard deviation of three independent experimental determinations. [b]k_{obs} is the observed pseudo-first-order rate constant for inhibition of 3 μM single-chain uPA by 6 μM PAI-1 and was calculated by analyses of Coomassie Brilliant Blue-stained gels as described in Experimental Procedures. [c]Significantly different from control in a t test with $p < 0.005$.

activity of the mature uPA enzyme than was reported for trypsinogen and small molecule substrates, differing only by 2−3 orders of magnitude (see Tables 1 and 4).

In spite of some early controversy over the relative activity of single-chain and two-chain uPA (*47*, *48*), it is now generally accepted that the activity of pro-uPA is approximately 10^4-fold lower than that of two-chain uPA. This zymogenicity factor should be compared to the activity difference between chymotrypsin and chymotrypsinogen or between trypsinogen and trypsin, which are between 10^6- and 10^8-fold (*49*). One possible explanation is that uPA differs from the other two proteases in lacking the consensus residues that make up the so-called zymogen triad that is thought to aid in stabilization of the zymogen by forming an extended hydrogen bond network that sequesters the side chain of Asp194, thus preventing maturation of the oxyanion hole (*3*, *29*). The greater inducible catalytic activity of pro-uPA by Ile-Ile and Ile-Val may very well be ascribed to the lack of a zymogen triad and imply that the oxyanion hole of single-chain uPA is not constrained in an inactive conformation but has the propensity to more easily switch between inactive and active conformations.

We also demonstrate that the dipeptides accelerate the reaction between pro-uPA and its primary serpin inhibitor PAI-1 20−50-fold above that of the intrinsic catalytic activity of the zymogen. Single-chain uPA was previously reported to have a slow but measurable reaction with PAI-1, leading to formation of a stable, SDS-resistant complex, even in the absence of dipeptides (*31*). Although the reaction is too slow to be of interest under physiological conditions, it is of considerable interest when trying to understand the molecular mechanisms regulating serine

Table 4: Effect of Dipeptides on the Inhibition of Single-Chain uPA and Two-Chain uPA by PAI-1[a]

protease	k_{lim} (s^{-1})	K_M (μM)	k_{lim}/K_M (M^{-1} s^{-1})	$\Delta G_T^{\ddagger b}$ (kcal/mol)
pro-uPA (without dipeptide)	0.003 ± 0.001	8.9 ± 3.8	$(3.5 \pm 1.6) \times 10^2$	14.0
pro-uPA (with Ile-Ile)	0.057 ± 0.004^c	13.8 ± 1.9	$(4.1 \pm 0.6) \times 10^{3c}$	12.5
pro-uPA (with Ile-Val)	0.14 ± 0.01^c	9.5 ± 1.7	$(1.5 \pm 0.3) \times 10^{4c}$	11.8
pro-uPA (with Asp-Val)	0.003 ± 0.0002	10.5 ± 1.5	$(3.2 \pm 0.5) \times 10^2$	14.0
tc-uPA (without dipeptide)	10.2 ± 0.3	2.2 ± 0.6	$(4.6 \pm 1.2) \times 10^6$	8.4
tc-uPA (with Ile-Ile)	10.4 ± 0.3	3.7 ± 0.2	$(2.8 \pm 0.2) \times 10^6$	8.7
tc-uPA (with Ile-Val)	7.4 ± 0.3^c	1.6 ± 0.2	$(4.5 \pm 0.6) \times 10^6$	8.4

[a]Data are reported as the best fit to the time-dependent fluorescence or stopped-flow data ± the standard error of the fit. The second-order rate constant for PAI-1 inhibition of proteases was calculated from the fitted fluorescence and stopped-flow data as k_{lim}/K_M. [b]Values for the transition state stabilization energy ($\Delta G_T^{\ddagger}$) were calculated from the k_{cat}/K_M values using the relationship $\Delta G_T^{\ddagger} = -RTln[(h/k_BT)(k_{cat}/K_M)]$, where k_B is Boltzmann's constant, h is Planck's constant, T is the temperature, and R is the gas constant. [c]Significantly different from control in a t test with $p < 0.005$.

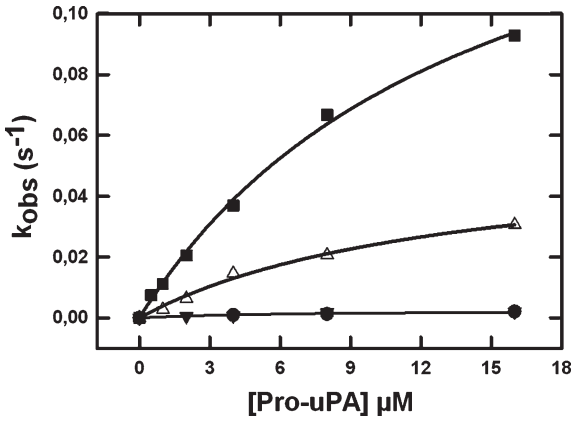

FIGURE 6: Formation of a complex between single-chain uPA and P9-NBD-PAI-1, as evaluated by spectrofluorometry. The rate of complex formation was determined at various single-chain uPA concentrations, in the presence of 50 nM P9-NBD-PAI-1 and with 50 mM of Ile-Val (■), Ile-Ile (△), and Asp-Val (●) or in the absence of dipeptides (▼). The reaction was followed over time with an excitation wavelength of 480 nm and an emission wavelength of 522 nm. Subsequently, the curves obtained were fit to a single-exponential equation, which provided k_{obs} values for each pro-uPA concentration. The dependence of the k_{obs} values on the pro-uPA concentration is described by a single rectangular hyperbola as detailed in Experimental Procedures and eq 4.

protease activity. Given the sensitivity of the fluorescent techniques used to determine the rate constants for PAI-1 inhibition, the observed approximately 10^4-fold reduced rate of inhibition for single-chain uPA may more appropriately reflect the intrinsic catalytic activity of pro-uPA against macromolecular substrates. The observation of an induction of enzyme activity as well as an increased rate of reaction with PAI-1 is in agreement with the fact that the early steps of the reactions of serine proteases with their serpin inhibitors resemble the reactions between enzyme and substrate. The formation of an SDS-resistant complex is based on the fact that at the acyl−enzyme intermediate stage, the serpin undergoes a conformational change, which is linked to deformation of the enzyme's active site and thereby halts the completion of the catalytic cycle (*45*, *50*, *51*). Thus, PAI-1 can be regarded as a macromolecular substrate in the sense that not only primary active site interactions but also extended binding interactions are considered during the reaction. In contrast to the 20−30-fold higher K_M values observed for reactions of dipeptide-activated pro-uPA compared to active, two-chain uPA with a tripeptide *p*-nitroanilide substrate, the disparity in K_M values was typically only 4-fold for PAI-1 reactions and no improvements in K_M were noted in the presence of the dipeptides (Table 4).

Nevertheless, the dipeptide-complexed single-chain uPA never becomes as active as two-chain uPA. The K_M for hydrolysis of a chromogenic substrate remained 20−30-fold higher than that for the two-chain form and the k_{cat} ~15−50-fold lower. Following a strategy reminiscent of one previously employed by Hedstrom et al. (*49*) when evaluating the effect of mutations of the N-terminus of trypsinogen, we found that the K_i values for competitive inhibition of dipeptide-complexed pro-uPA by PAB, amiloride, and upain-1 were much higher than those for inhibition of two-chain uPA. The poor inhibition by PAB and amiloride can most readily be interpreted as incomplete maturation of the S1 subsite, as the main contacts between these inhibitors and uPA are made within this pocket (*52*). Upain-1 has a more extended interaction surface with uPA but still binds poorly to the zymogen form (*38*, *41*). Thus, the question remaining after this study, the work of Bode and Huber (*4*), and others (*6*, *7*, *10*, *12*) is why the single-chain enzyme does not acquire full activity even with optimal dipeptide concentrations. Bulaj and Otlewski (*10*) have shown that although the Ile-Val dipeptide adduct of trypsinogen gains structural stability similar to that of the active enzyme, effects on k_{cat}/K_M are marginal. Obviously, cleavage of the activation loop induces subtle conformational changes in addition to those that can be ascribed to the insertion of the new N-terminus. Pasternak et al. (*28*) have suggested that the removal of the sequences around the peptide bond that is cleaved upon activation, particularly Lys158, contributes to the activation of trypsinogen. The presence of the activation peptide in the uncleaved form could sterically retard the formation of the active conformation, or the stabilization of the active conformation could require the activation peptide to be constrained in a particular conformation that can only be attained after cleavage. This may be a more general mechanism of zymogen activation also applicable to uPA and explain why the full activity of single-chain uPA or trypsinogen is not obtained when a dipeptide mimic of the N-terminal residues induces a seemingly active conformation. However, in this case, Lys158 does not seem to be the residue responsible for decreased activity, since the mutant lacking this residue, K158A pro-uPA, has less activity than wild-type pro-uPA when induced by dipeptides.

Some serine proteases do not acquire full activity even in the cleaved two-chain form before being bound by a cofactor. For example, in the case of Factor VIIa, full activity is only attained after the protease is bound by tissue factor, which acts to induce the mature conformation of the catalytic site (*53*). Thus, structure−function aspects other than the basic insertion of the N-terminal residues seem to be important for stabilization of the active conformation. Bode and Huber have explained the

difference between a free and a covalently bound amino terminus in terms of increased effective concentration, a reduction in rotational and translational freedom, and orientation such that a covalently bound amino terminus may more easily confer activity as compared to free peptides (*4*). Inclusion of the zymogen-specific mAb-112 or FAb-112 in the peptidolytic and PAI-1 inhibition experiments was a means of evaluating the conformational flexibility of the activation domain, specifically the oxyanion hole and the autolysis loop where we have previously localized the epitope for mAb-112 (*37*). Given that mAb-112 or FAb-112 binds to the zymogen form of uPA with an affinity several orders of magnitude greater than that of active uPA, the observation of near-complete inhibition of catalytic activity in the presence of the antibody suggests that the conformational equilibrium of the autolysis loop is shifted more toward a zymogen-like state than an active state. Thus, it is reasonable to suggest that in the absence of activation loop cleavage, the dipeptide-activated zymogen remains more flexible, lacking the rigid structure of active uPA. In terms of the effects of dipeptide in reducing the transition state stabilization energy ($\Delta G_T^{\ddagger}$), reactions with a peptidolytic substrate or the serpin inhibitor PAI-1 were found to be similar, with the dipeptide adducts having $\Delta G_T^{\ddagger}$ values destabilized by ~4−5 kcal/mol as determined by calculating the $\Delta\Delta G_T^{\ddagger}$ from the k_{cat}/K_M or k_{lim}/K_M ratios relative to those of active uPA (see Tables 1 and 4). This notion is therefore consistent with an increased flexibility of zymogen−dipeptide adducts and the presence of a significant energy barrier to efficient catalysis at the level of the mature protease.

We have capitalized upon the dipeptide activation of pro-uPA to label the active site with dansyl-EGR-cmk. Following removal of the dipeptide, the enzyme returned completely to the inactive zymogen form as judged by its high affinity for a monoclonal antibody specific for the zymogen, mAb-112 (*37*). Activation of the single-chain form by proteolytic cleavage with plasmin was coupled to a quench and a red shift of the fluorescence emission spectrum. Notably, the same shift was produced by the activating dipeptides such that 50 mM Ile-Ile shifted the fluorescence emission spectrum almost totally to that of dansyl-EGR-cmk-labeled two-chain uPA. This observation is at first sight in disagreement with the fact that the enzyme activity of the dipeptide-activated pro-uPA remained much lower than that of two-chain uPA. In fact, the dipeptide concentration needed to produce an optimal effect on the enzyme activity of single-chain uPA was considerably higher than that needed to produce an optimal effect on the spectrum. One potential explanation is that the equilibrium between active and inactive forms is more easily shifted toward the active form when the active site is derivatized with a transition state inhibitor such as the peptidyl chloromethylketone inhibitor used in these studies. This interpretation is in agreement with the findings by Bode and Huber that trypsin inhibitors can pull the conformation of trypsinogen toward that of trypsin (*5*, *6*). Furthermore, the sensitivity of the fluorescent probe, when covalently coupled to the active site of pro-uPA, may not have the resolution required to identify very small conformational changes that could have profound effects on enzyme activity. Protease stabilization by the hemiketal adduct can be considered in terms of an increase in the effective concentration due to the covalent nature of interaction. It is therefore intriguing to speculate that in the presence of high concentrations of substrate we would observe such an effect; however, high concentrations of the tripeptide *p*-nitroanilide substrate were difficult to obtain due to limitations of solubility. Nonetheless, in the PAI-1 inhibition experiments, where we were able to obtain high concentrations of protease under pseudo-first-order conditions, we obtained second-order rate constants that were a full order of magnitude greater than those obtained with the tripeptide *p*-nitroanilide substrate. These findings suggest a possible advantage of further conformational stabilization by the extended interactions of the serpin with the protease, which are lacking with the small molecule substrate.

On the basis of the structure and fold of staphylocoagulase, a new family of bifunctional bacterial zymogen activator and adhesion proteins (ZAAPs) has been identified, including von Willebrand factor binding protein (vWbp) that also nonproteolytically activates prothrombin (*54*). This family has expanded the number of zymogen activators utilizing a mechanism different from activation by proteolysis but whose specific functions remain to be learned. These findings indicate that catalytic activity in the zymogen form of uPA can be induced by peptides sequentially similar to the N-terminus of the two-chain active protease. It has been determined that plasminogen activators, streptokinase and staphylokinase, occur in both streptococcal and staphylococcal strains. Therefore, it is conceivable that nonproteolytic conformational activators of other serine proteases such as single-chain uPA may exist naturally and function to circumvent the normal regulatory steps, altering substrate and inhibitor specificities and localizing these activities to new sites.

In conclusion, we have demonstrated that dipeptides can induce genuine enzyme activity in a single-chain form of uPA in a manner reminiscent of the dipeptide activation of trypsinogen, but with a greater enhancement of catalytic activity relative to the mature protease. Additionally, we have for the first time evaluated kinetically the inhibition of pro-uPA by PAI-1, further illustrating that the presence of extended molecular interactions is linked to improved catalysis by dipeptide activators. Nevertheless, the active site of the single-chain enzyme, even in the presence of saturating concentrations of the dipeptide, remains different and less catalytically efficient than that of the two-chain form, likely due to an increase in flexibility and an equilibrium shift toward that of the zymogen. Moreover, addition of the dipeptides provides a novel means of covalently coupling a fluorescent probe to pro-uPA at residues potentially forming the active site, further permitting direct observation of conformational changes within the protease domain and following conformational transitions during zymogen activation.

REFERENCES

1. Neurath, H. (1984) Evolution of proteolytic enzymes. *Science 224*, 350–357.
2. Hedstrom, L. (2002) Serine protease mechanism and specificity. *Chem. Rev. 102*, 4501–4524.
3. Madison, E. L., Kobe, A., Gething, M. J., Sambrook, J. F., and Goldsmith, E. J. (1993) Converting tissue plasminogen activator to a zymogen: A regulatory triad of Asp-His-Ser. *Science 262*, 419–421.
4. Bode, W., and Huber, R. (1976) Induction of the bovine trypsinogen-trypsin transition by peptides sequentially similar to the N-terminus of trypsin. *FEBS Lett. 68*, 231–236.
5. Bode, W., Schwager, P., and Huber, R. (1978) The transition of bovine trypsinogen to a trypsin-like state upon strong ligand binding. The refined crystal structures of the bovine trypsinogen-pancreatic trypsin inhibitor complex and of its ternary complex with Ile-Val at 1.9 Å resolution. *J. Mol. Biol. 118*, 99–112.
6. Bode, W. (1979) The transition of bovine trypsinogen to a trypsin-like state upon strong ligand binding. II. The binding of the pancreatic trypsin inhibitor and of isoleucine-valine and of sequentially related peptides to trypsinogen and to p-guanidinobenzoate-trypsinogen. *J. Mol. Biol. 127*, 357–374.

7. Antonini, E., Ascenzi, P., Bolognesi, M., Guarneri, M., Menegatti, E., and Amiconi, G. (1984) Catalytic and ligand binding properties of bovine trypsinogen and its complex with the effector dipeptide Ile-Val. A comparative study. *Mol. Cell. Biochem. 60*, 163–181.
8. Ascenzi, P., Amiconi, G., Bolognesi, M., Menegatti, E., and Guarneri, M. (1987) Binding of the Ile-Val and Val-Val effector dipeptides to the binary adducts of bovine trypsinogen with Kunitz and Kazal inhibitors as well as the acylating agent p-nitrophenyl p-guanidinobenzoate. A thermodynamic and kinetic study. *J. Mol. Biol. 194*, 751–754.
9. Bulaj, G., and Otlewski, J. (1994) Denaturation of free and complexed bovine trypsinogen with the calcium ion, dipeptide Ile-Val and basic pancreatic trypsin inhibitor (Kunitz). *Eur. J. Biochem. 223*, 939–946.
10. Bulaj, G., and Otlewski, J. (1995) Ligand-induced changes in the conformational stability of bovine trypsinogen and their implications for the protein function. *J. Mol. Biol. 247*, 701–716.
11. Coletta, M., Ascenzi, P., Amiconi, G., Bolognesi, M., Guarneri, M., and Menegatti, E. (1990) Bovine trypsinogen activation. A thermodynamic study. *Biophys. Chem. 37*, 355–362.
12. Menegatti, E., Guarneri, M., Bolognesi, M., Ascenzi, P., and Amiconi, G. (1985) Activating effect of the Ile-Val dipeptide on the catalytic properties of bovine trypsinogen. *Biochim. Biophys. Acta 832*, 1–6.
13. Friedrich, R., Panizzi, P., Fuentes-Prior, P., Richter, K., Verhamme, I., Anderson, P. J., Kawabata, S., Huber, R., Bode, W., and Bock, P. E. (2003) Staphylocoagulase is a prototype for the mechanism of cofactor-induced zymogen activation. *Nature 425*, 535–539.
14. Boxrud, P. D., Verhamme, I. M., Fay, W. P., and Bock, P. E. (2001) Streptokinase triggers conformational activation of plasminogen through specific interactions of the amino-terminal sequence and stabilizes the active zymogen conformation. *J. Biol. Chem. 276*, 26084–26089.
15. Wang, S., Reed, G. L., and Hedstrom, L. (1999) Deletion of Ile1 changes the mechanism of streptokinase: Evidence for the molecular sexuality hypothesis. *Biochemistry 38*, 5232–5240.
16. Boxrud, P. D., and Bock, P. E. (2004) Coupling of conformational and proteolytic activation in the kinetic mechanism of plasminogen activation by streptokinase. *J. Biol. Chem. 279*, 36642–36649.
17. Boxrud, P. D., Fay, W. P., and Bock, P. E. (2000) Streptokinase binds to human plasmin with high affinity, perturbs the plasmin active site, and induces expression of a substrate recognition exosite for plasminogen. *J. Biol. Chem. 275*, 14579–14589.
18. Boxrud, P. D., Verhamme, I. M., and Bock, P. E. (2004) Resolution of conformational activation in the kinetic mechanism of plasminogen activation by streptokinase. *J. Biol. Chem. 279*, 36633–36641.
19. Boxrud, P. D., Verhamme, I. M., Fay, W. P., and Bock, P. E. (2001) Streptokinase triggers conformational activation of plasminogen through specific interactions of the amino-terminal sequence and stabilizes the active zymogen conformation. *J. Biol. Chem. 276*, 26084–26089.
20. Andreasen, P. A., Egelund, R., and Petersen, H. H. (2000) The plasminogen activation system in tumor growth, invasion, and metastasis. *Cell. Mol. Life Sci. 57*, 25–40.
21. Nielsen, L. S., Hansen, J. G., Skriver, L., Wilson, E. L., Kaltoft, K., Zeuthen, J., and Dano, K. (1982) Purification of zymogen to plasminogen activator from human glioblastoma cells by affinity chromatography with monoclonal antibody. *Biochemistry 21*, 6410–6415.
22. Skriver, L., Nielsen, L. S., Stephens, R., and Dano, K. (1982) Plasminogen activator released as inactive proenzyme from murine cells transformed by sarcoma virus. *Eur. J. Biochem. 124*, 409–414.
23. Wun, T. C., Ossowski, L., and Reich, E. (1982) A proenzyme form of human urokinase. *J. Biol. Chem. 257*, 7262–7268.
24. Kielberg, V., Andreasen, P. A., Grondahl-Hansen, J., Nielsen, L. S., Skriver, L., and Dano, K. (1985) Proenzyme to urokinase-type plasminogen activator in the mouse in vivo. *FEBS Lett. 182*, 441–445.
25. List, K., Jensen, O. N., Bugge, T. H., Lund, L. R., Ploug, M., Dano, K., and Behrendt, N. (2000) Plasminogen-independent initiation of the pro-urokinase activation cascade in vivo. Activation of pro-urokinase by glandular kallikrein (mGK-6) in plasminogen-deficient mice. *Biochemistry 39*, 508–515.
26. Kilpatrick, L. M., Harris, R. L., Owen, K. A., Bass, R., Ghorayeb, C., Bar-Or, A., and Ellis, V. (2006) Initiation of plasminogen activation on the surface of monocytes expressing the type II transmembrane serine protease matriptase. *Blood 108*, 2616–2623.
27. Moran, P., Li, W., Fan, B., Vij, R., Eigenbrot, C., and Kirchhofer, D. (2006) Pro-urokinase-type plasminogen activator is a substrate for hepsin. *J. Biol. Chem. 281*, 30439–30446.
28. Pasternak, A., Liu, X., Lin, T. Y., and Hedstrom, L. (1998) Activating a zymogen without proteolytic processing: Mutation of Lys15 and Asn194 activates trypsinogen. *Biochemistry 37*, 16201–16210.
29. Xue, Y. M., Zhu, H., Shi, W., Liu, W., Liu, J. N., and Ma, Z. (2000) Construction and Characterization of a Mutant of Single-chain Urokinase-type Plasminogen Activator Ser(175)-His(187)-mscu-PA. *Acta Biochim. Biophys. Sin. 32*, 26–30.
30. Andreasen, P. A., Nielsen, L. S., Kristensen, P., Grondahl-Hansen, J., Skriver, L., and Dano, K. (1986) Plasminogen activator inhibitor from human fibrosarcoma cells binds urokinase-type plasminogen activator, but not its proenzyme. *J. Biol. Chem. 261*, 7644–7651.
31. Behrendt, N., List, K., Andreasen, P. A., and Dano, K. (2003) The pro-urokinase plasminogen-activation system in the presence of serpin-type inhibitors and the urokinase receptor: Rescue of activity through reciprocal pro-enzyme activation. *Biochem. J. 371*, 277–287.
32. Madsen, M. A., Deryugina, E. I., Niessen, S., Cravatt, B. F., and Quigley, J. P. (2006) Activity-based protein profiling implicates urokinase activation as a key step in human fibrosarcoma intravasation. *J. Biol. Chem. 281*, 15997–16005.
33. Petersen, H. H., Hansen, M., Schousboe, S. L., and Andreasen, P. A. (2001) Localization of epitopes for monoclonal antibodies to urokinase-type plasminogen activator: Relationship between epitope localization and effects of antibodies on molecular interactions of the enzyme. *Eur. J. Biochem. 268*, 4430–4439.
34. Dupont, D. M., Blouse, G. E., Hansen, M., Mathiasen, L., Kjelgaard, S., Jensen, J. K., Christensen, A., Gils, A., Declerck, P. J., Andreasen, P. A., and Wind, T. (2006) Evidence for a pre-latent form of the serpin plasminogen activator inhibitor-1 with a detached β-strand 1C. *J. Biol. Chem. 281*, 36071–36081.
35. Wind, T., Jensen, J. K., Dupont, D. M., Kulig, P., and Andreasen, P. A. (2003) Mutational analysis of plasminogen activator inhibitor-1. *Eur. J. Biochem. 270*, 1680–1688.
36. Blouse, G. E., Perron, M. J., Kvassman, J. O., Yunus, S., Thompson, J. H., Betts, R. L., Lutter, L. C., and Shore, J. D. (2003) Mutation of the highly conserved tryptophan in the serpin breach region alters the inhibitory mechanism of plasminogen activator inhibitor-1. *Biochemistry 42*, 12260–12272.
37. Blouse, G. E., Bøtkjær, K. A., Deryugina, E., Byszuk, A. A., Jensen, J. M., Mortensen, K. K., Quigley, J. P., and Andreasen, P. A. (2009) A novel mode of intervention with serine protease activity: Targeting zymogen activation. *J. Biol. Chem. 284*, 4647–4657.
38. Hansen, M., Wind, T., Blouse, G. E., Christensen, A., Petersen, H. H., Kjelgaard, S., Mathiasen, L., Holtet, T. L., and Andreasen, P. A. (2005) A urokinase-type plasminogen activator-inhibiting cyclic peptide with an unusual P2 residue and an extended protease binding surface demonstrates new modalities for enzyme inhibition. *J. Biol. Chem. 280*, 38424–38437.
39. Markwardt, F., Landmann, H., and Walsmann, P. (1968) Comparative studies on the inhibition of trypsin, plasmin, and thrombin by derivatives of benzylamine and benzamidine. *Eur. J. Biochem. 6*, 502–506.
40. Vassalli, J. D., and Belin, D. (1987) Amiloride selectively inhibits the urokinase-type plasminogen activator. *FEBS Lett. 214*, 187–191.
41. Zhao, G., Yuan, C., Wind, T., Huang, Z., Andreasen, P. A., and Huang, M. (2007) Structural basis of specificity of a peptidyl urokinase inhibitor, upain-1. *J. Struct. Biol. 160*, 1–10.
42. Bock, P. E., Day, D. E., Verhamme, I. M., Bernardo, M. M., Olson, S. T., and Shore, J. D. (1996) Analogs of human plasminogen that are labeled with fluorescence probes at the catalytic site of the zymogen. Preparation, characterization, and interaction with streptokinase. *J. Biol. Chem. 271*, 1072–1080.
43. Panizzi, P., Friedrich, R., Fuentes-Prior, P., Kroh, H. K., Briggs, J., Tans, G., Bode, W., and Bock, P. E. (2006) Novel fluorescent prothrombin analogs as probes of staphylocoagulase-prothrombin interactions. *J. Biol. Chem. 281*, 1169–1178.
44. Andreasen, P. A., Georg, B., Lund, L. R., Riccio, A., and Stacey, S. N. (1990) Plasminogen activator inhibitors: Hormonally regulated serpins. *Mol. Cell. Endocrinol. 68*, 1–19.
45. Huntington, J. A. (2006) Shape-shifting serpins: Advantages of a mobile mechanism. *Trends Biochem. Sci. 31*, 427–435.
46. Shore, J. D., Day, D. E., Francis-Chmura, A. M., Verhamme, I., Kvassman, J., Lawrence, D. A., and Ginsburg, D. (1995) A fluorescent probe study of plasminogen activator inhibitor-1. Evidence for reactive center loop insertion and its role in the inhibitory mechanism. *J. Biol. Chem. 270*, 5395–5398.
47. Petersen, L. C., Lund, L. R., Nielsen, L. S., Dano, K., and Skriver, L. (1988) One-chain urokinase-type plasminogen activator from human sarcoma cells is a proenzyme with little or no intrinsic activity. *J. Biol. Chem. 263*, 11189–11195.
48. Collen, D., Zamarron, C., Lijnen, H. R., and Hoylaerts, M. (1986) Activation of plasminogen by pro-urokinase. II. Kinetics. *J. Biol. Chem. 261*, 1259–1266.

49. Hedstrom, L., Lin, T. Y., and Fast, W. (1996) Hydrophobic interactions control zymogen activation in the trypsin family of serine proteases. *Biochemistry 35*, 4515–4523.
50. Ye, S., and Goldsmith, E. J. (2001) Serpins and other covalent protease inhibitors. *Curr. Opin. Struct. Biol. 11*, 740–745.
51. Dupont, D. M., Madsen, J. B., Kristensen, T., Bodker, J. S., Blouse, G. E., Wind, T., and Andreasen, P. A. (2009) Biochemical properties of plasminogen activator inhibitor-1. *Front. Biosci.,* 1337–1361.
52. Zeslawska, E., Schweinitz, A., Karcher, A., Sondermann, P., Sperl, S., Sturzebecher, J., and Jacob, U. (2000) Crystals of the urokinase type plasminogen activator variant β(c)-uPAin complex with small molecule inhibitors open the way towards structure-based drug design. *J. Mol. Biol. 301*, 465–475.
53. Osterud, B., and Rapaport, S. I. (1977) Activation of factor IX by the reaction product of tissue factor and factor VII: Additional pathway for initiating blood coagulation. *Proc. Natl. Acad. Sci. U.S.A. 74*, 5260–5264.
54. Panizzi, P., Friedrich, R., Fuentes-Prior, P., Bode, W., and Bock, P. E. (2004) The staphylocoagulase family of zymogen activator and adhesion proteins. *Cell. Mol. Life Sci. 61*, 2793–2798.
55. Pjura, P. E., Lenhoff, A. M., Leonard, S. A., and Gittis, A. G. (2000) Protein crystallization by design: Chymotrypsinogen without precipitants. *J. Mol. Biol. 300*, 235–239.
56. Ghani, U., Ng, K. K., Atta ur, R., Choudhary, M. I., Ullah, N., and James, M. N. (2001) Crystal structure of γ-chymotrypsin in complex with 7-hydroxycoumarin. *J. Mol. Biol. 314*, 519–525.